Available online at www.sciencedirect.com
ScienceDirect
Journal of Crystal Growth 310 (2008) 313–317
JOURNAL OF CRYSTAL GROWTH
www.elsevier.com/locate/jcrysgro

Improvement of luminescence from Si nanocrystals with thermal annealing in CO_2

M.D. Yang[a], A.H.M. Chu[a], J.L. Shen[a,*], Y.H. Huang[b], T.N. Yang[b], M.C. Chen[b], C.C. Chiang[b], S.M. Lan[b], W.C. Chou[c], Y.C. Lee[d]

[a]*Department of Physics, Center for Nanotechnology at CYCU and R&D Center for Membrane Technology, Chung Yuan Christian University, Chung-Li, Taiwan, ROC*
[b]*Institute of Nuclear Energy Research Atomic Energy Council, Long-Tan, Taiwan, ROC*
[c]*Electrophysics Department, National Chiao-Tung University, Hsin-Chu, Taiwan, ROC*
[d]*Department of Electronic Engineering, Tung Nan Institute of Technology, Taipei, Taiwan, ROC*

Received 18 July 2007; received in revised form 26 October 2007; accepted 28 October 2007
Communicated by K. Nakajima
Available online 5 November 2007

Abstract

Photoluminescence (PL) of Si nanocrystals with annealing in CO_2 was studied using the continuous and time-resolved PL measurements. The PL intensity enhances as annealing temperature increases, which is attributed to passivation of the nonradiative recombination centers. As the annealing temperature is 950 °C the PL intensity has a maximum value, which increases about a factor of 3 than that of the untreated sample. Based on the emission energy dependence of the PL decay time, the depth of carrier localization is found to increase after the annealing in CO_2. We suggest that the oxygen atoms desorbed from CO_2 diffuse to react with Si nanocrystals and introduce localized states at the Si/SiO_2 interface.

PACS: 78.55.−m; 78.67.Ch; 78.68.+m

Keywords: A1. Nanoclusters; A3. Chemical vapor deposition processes; B2. Semiconducting silicon

1. Introduction

Many attempts have been made to produce visible luminescence from Si-based nanostructures, such as porous silicon [1,2] and silicon nanocrystals [3,4]. In particular, silicon nanocrystals embedded in SiO_2 matrix are receiving widespread interest because of their emission energy can cover the range from infrared to visible light. Moreover, the growth of silicon nanocrystals can be compatible with common integrated circuits for fabricating various optoelectronic and high-speed electronic devices. There are several techniques to produce silicon nanocrystals, for example, ion implantation [5,6], sputtering [7], e-beam evaporation [8]. However, a significant fraction of the interface or surface defects are produced during the growth processes and radiative yield of the silicon nanocrystals is hence reduced. It have been reported that annealing the silicon nanocrystals with hydrogen [9], oxygen [10], nitrogen [11] and forming gas [12] can increase its photoluminescence (PL) efficiency, which is attributed to the passivation of defects at the interface or surface.

It is well known that the time-resolved PL gives direct information on the luminescence decay mechanism. Carrier lifetimes obtained from time-resolved PL provide not only a fundamental insight in the luminescence mechanism but also the possibility to engineer nanostructures optimized for device applications. In this study, we study the PL from silicon nanocrystals embedded in SiO_2 matrix that were annealed in CO_2. With increasing the annealing temperature in CO_2, both the PL intensity and PL decay time increase. These behaviors can be explained by passivation

*Corresponding author.
E-mail address: jlshen@cycu.edu.tw (J.L. Shen).

0022-0248/$ - see front matter © 2007 Elsevier B.V. All rights reserved.
doi:10.1016/j.jcrysgro.2007.10.074

of the nonradiative recombination centers by oxygen. We also found that the depth of carrier localization increases as annealing temperature increases.

2. Experimental details

An atmospheric pressure chemical vapor deposition (APCVD) system was used to produce the silicon nanocrystals embedded in SiO_2 matrix. SiH_2Cl_2 and N_2O gases were introduced into the atmospheric pressure chamber by N_2, with the ratio of SiH_2Cl_2 to N_2O is 1.56. SiO_2 matrix was deposited on a p^+-Si (1 1 1) substrate at 950 °C and subsequently the excess Si atoms were self-assembled in the matrix in the form of cluster, and nucleated by annealing in N_2 at 1150 °C for 30 min. Finally, the samples were annealed in CO_2 ranging from 875 to 950 °C for 1 h. Fig. 1(a) shows the high-resolution transmission electron (HRTEM) micrograph of the Si nanocrystals grown by APCVD. Si nanocrystals were clearly observed to be embedded in Si oxide matrix. The sizes of Si nanocrystals were in the range 4–5 nm. The PL measurements were carried out using an Ar^+ laser (488 nm). Time-resolved PL spectra were measured using a pulsed Nd:YAG laser with a pulse duration 5 ns and a repetition rate 10 Hz as an excitation source. The collected PL was directly projected into a grating spectrometer and then detected with a photomultiplier tube (PMT).

3. Results and discussion

Fig. 2 shows the room temperature PL spectra of the silicon nanocrystals under different annealing temperature in CO_2. The PL peak energies in Fig. 2 are about 1.7 eV, similar to those in previous studies [6,13]. The inset shows the PL intensity as a function of annealing temperature in CO_2. It is found the PL intensity increases with the annealing temperature. Especially, as the annealing is 950 °C the PL intensity has a maximum value, which increases about a factor of 3 than that of the untreated sample. The annealing in CO_2 also leads to a blueshift of the PL spectrum from 1.7 to 1.75 eV, as shown in Fig. 2. Since the PL peak energy depends on the nanocrystal size, the blueshift could result from a reduction of the size of Si nanocrystals during the annealing processes. Indeed, the HRTEM images for the samples annealed in 925 and 950 °C reveal that the sizes of Si nanocrystals with annealing are smaller than those of the untreated Si nanocrystals, as shown in Figs. 1(b) and (c). It is known that the CO_2 dissociates to form CO and O during thermal annealing [14]; the former desorbs at 400 K and the residual oxygen atom can react with silicon nanocrystals. We therefore suggest that the produced oxygen atoms react with Si bonds of Si nanocrystal and terminated the dangling bonds. This reaction has a direct effect on the effective size of Si nanocrystals and shifts the PL peak. It is noted that the diffusion length of oxygen atoms for our annealing temperatures (875–950 °C) was roughly estimated to be ~15–40 nm from the oxidation of Si in oxygen [15]. In our case, this length is sufficient for the oxygen atoms to diffuse and react with silicon nanocrystals, influencing the luminescence properties.

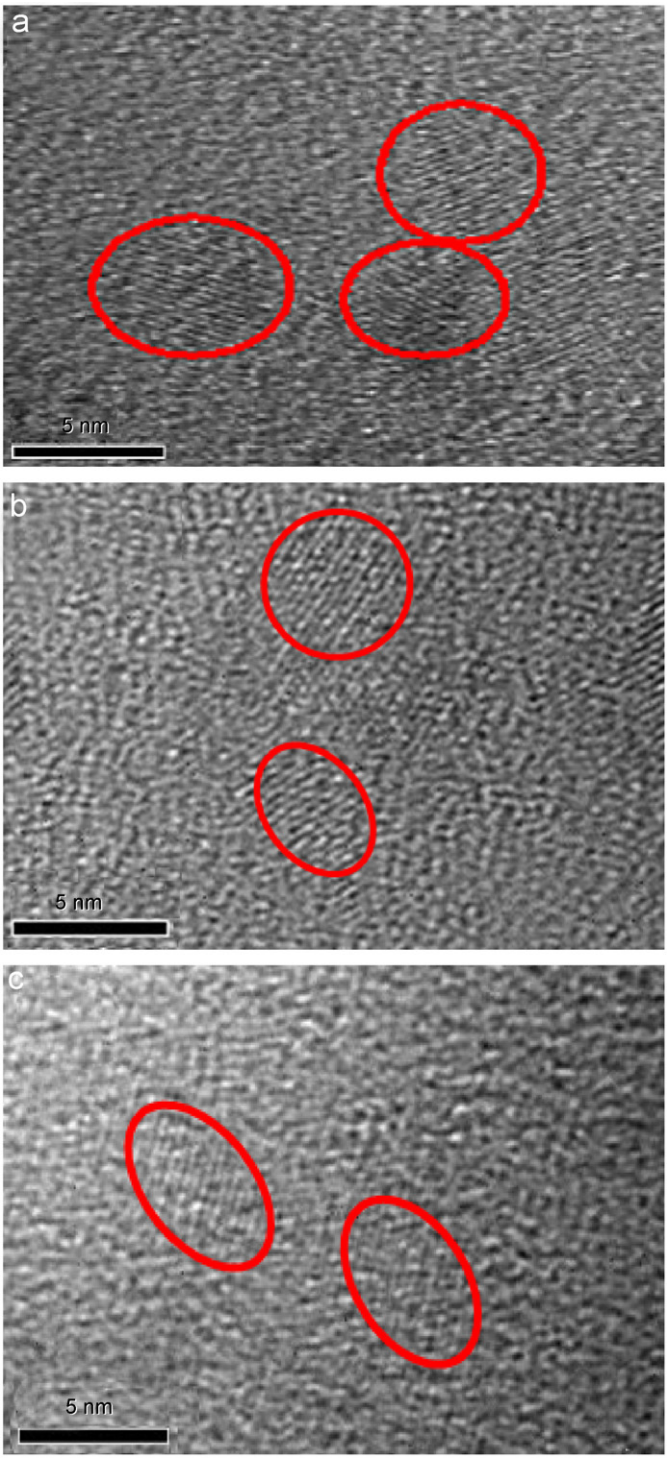

Fig. 1. High-resolution transmission electron microscopy (HRTEM) image for the: (a) untreated Si nanocrystals; (b) annealed Si nanocrystals with 925 °C; and (c) annealed Si nanocrystals with 950 °C.

The PL enhancement after annealing in CO_2 may arise from the increase of radiative processes (quantum yield) or

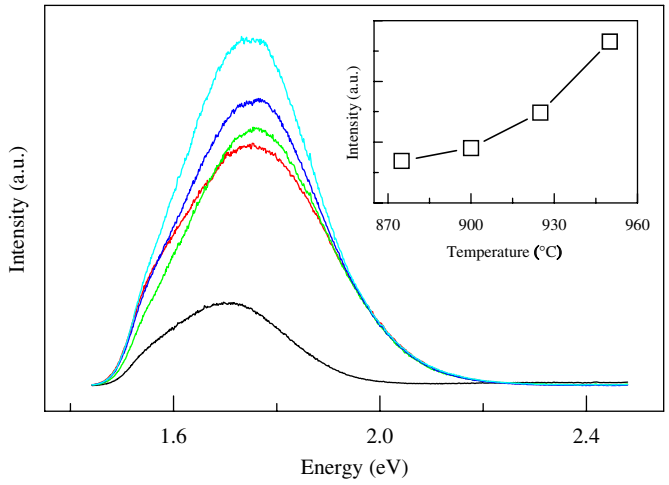

Fig. 2. The PL spectra of Si nanocrystals annealed in CO_2 with different annealing temperatures. The annealing temperature from bottom to top is the untreated, 875, 900, 925, and 950 °C, respectively. The inset shows the PL intensity as a function of annealing temperature.

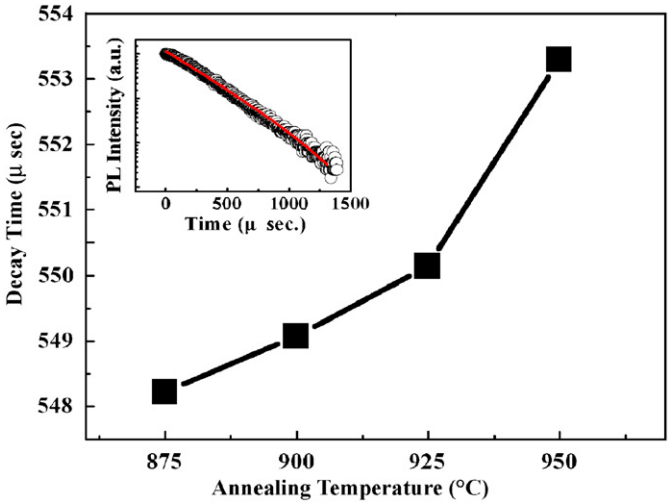

Fig. 3. The decay time of Si nanocrystals annealed in CO_2 with different temperatures. The line is a guide for the eye. The inset shows PL decay profile of Si nanocrystals without annealing.

the decrease of nonradiative processes. In order to find out the origin of PL enhancement, the time-resolved PL measurements were performed. The 1.7 eV PL decay profile of Si nanocrystals without annealing is shown in the inset of Fig. 3, indicating a single exponential decay over three-orders of magnitude. The evolution of the PL decay can be described by an exponential function

$$I(t) = I_0 \exp(-t/\tau), \quad (1)$$

where τ represents the measured PL decay time, I_0 represents the amplitude of the PL intensity at time $t = 0$. The solid line in the inset shows the fitted result using Eq. (1), giving a value of $\tau = 548\,\mu s$ for the decay time. The PL decay time τ of Si nanocrystals as a function of annealing temperature is plotted in Fig. 3. The PL decay time increases as the annealing temperature increases. The measured PL decay time τ can be related to the time constants for the radiative and nonradiative recombination τ_R and τ_{NR}, respectively, as follows:

$$1/\tau = 1/\tau_R + 1/\tau_{NR}. \quad (2)$$

Generally speaking, the PL intensity I can be simply given by

$$I \propto \tau/\tau_R. \quad (3)$$

Fig. 4 plots the PL intensity I versus the PL decay time τ for Si nanocrystals with various annealing temperatures. It is found that the PL intensity is proportional to the PL decay time, displayed as the solid line in Fig. 4. According to Eq. (3) the proportionality of PL intensity I and PL decay time τ indicates τ_R remain unchanged by the annealing in CO_2. In other words, nonradiative recombination centers are expected to change during the annealing processes. We therefore deduce that the increase of the PL intensity and decay time after annealing are due to the passivation of nonradiative recombination centers.

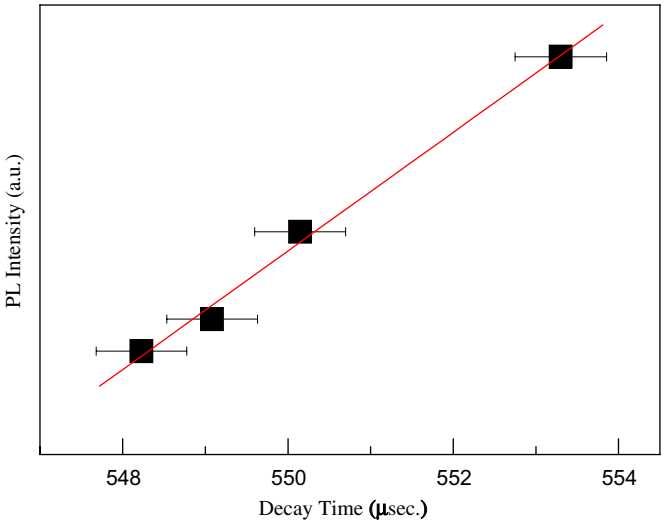

Fig. 4. The PL intensity I versus the PL decay time τ for Si nanocrystals with various annealing temperatures. The line reveals that the PL intensity is proportional to the PL decay time.

It is well known that the dangling bonds or/and interface defects can trap the photoexcited carriers and lead to the nonradiative recombination [16]. We therefore suggest that the oxygen atoms dissociated from the CO_2 annealing passivate the dangling bonds, leading to the enhancement of quantum yield (PL intensity). Recently Wolkin et al. [17] demonstrated that the incorporation of oxygen atoms can create the Si=O covalent bonds at the Si/SiO_2 interface. On the other hand, formation of the Si–O–Si bonds (single bonds) at the Si nanocrystal surface has also been reported by Vasiliev et al. [18] as oxygen is introduced to Si nanocrystals. Thus, the Si=O bonds and/or the Si–O–Si bonds may be formed at the Si/SiO_2 interface during the CO_2 annealing, terminating the dangling bonds. With the decrease of nonradiative recombination, the photoexcited

carriers diffuse over a long distance and survive longer. This effect results in a longer PL decay time, as displayed in Fig. 3.

The open circles in Fig. 5 show the measured lifetimes as a function of emission energy for Si nanocrystals annealed at 900 °C. The lifetime of PL decay decreases as the emission energy increases, which is a characteristic of carrier localization. Similar behavior has been observed for other samples. Localization due to the surface states or structural disorder may generate localized sites with different energies. Accordingly, localized carriers can be transferred from higher-energy sites to lower-energy sites through a relaxation process. [19] The decay rate of localized carriers is expressed as the radiative recombination rate and the transfer rate to lower-energy sites. Thus, the observed lifetime decreases as the emission energy increases. The combination of recombination and transfer has been modeled by assuming the density of localized tail states is proportional to $\exp(-E/E_0)$, where E_0 describes the amount of spreading in the density of states. The relationship between lifetime $\tau(E)$ and PL energy E with the function [19]:

$$\tau(E) = \frac{\tau_{rad}}{1 + \exp[(E - E_{me})/E_0]}, \quad (4)$$

where E_{me} is defined by a definite energy for which the decay time equals the transfer time, and E_0 is the depth of the localized states. τ described by Eq. (4) is plotted with the dashed line in Fig. 5. A good fit to experiment confirms the existence of carrier localization. From the fitting curve, τ_{rad}, E_{me}, and E_0 are estimated to be 702 μs, 1.89 eV, and 25 meV, respectively.

Fig. 6 displays the depth of the localized states E_0 as a function of annealing temperature. E_0 was found to increase as the annealing temperature is increased. The increase of E_0 reveals that the degree of carrier localization increases as the annealing temperature is increased. As

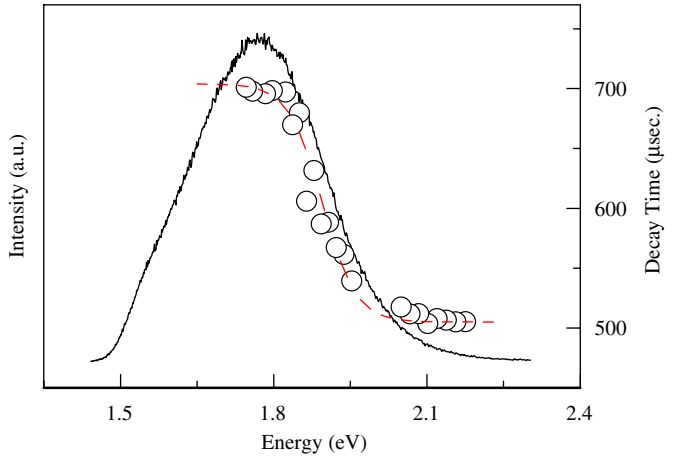

Fig. 5. The open circles show emission energy dependence of τ for Si nanocrystals annealed at 900 °C. The dashed line displays the calculated result using Eq. (4). The PL intensity is also displayed (solid line).

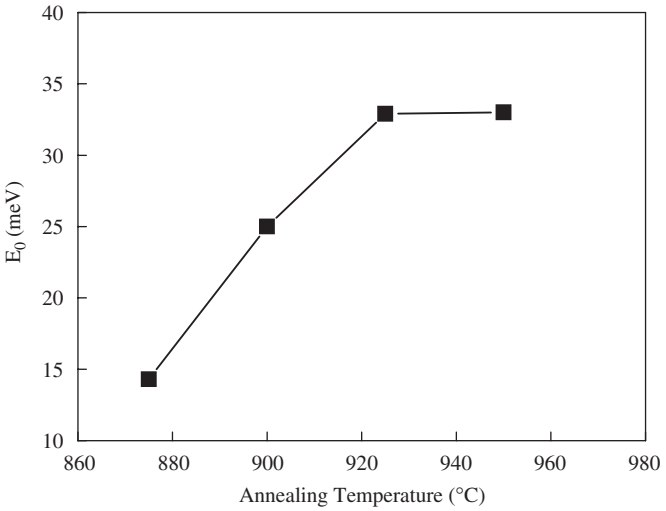

Fig. 6. The depth of the localized states E_0 as a function of annealing temperature. The line is a guide for the eye.

mentioned above, the Si═O bonds and/or the Si–O–Si bonds are likely to be formed at the Si/SiO_2 interface during the CO_2 annealing. The photoexcited carriers may thus be localized on the Si═O bonds and/or the Si–O–Si bonds. However, based on simulation of Wolkin et al. [17] there are no trap states for the large size of nanocrystals (diameter > 3 nm). Since the sizes of our Si nanocrystals are in the range 4–5 nm, the localized states originated from the Si═O bonds should be ruled out. We therefore suggest that the photoexcited carriers are localized on the Si–O–Si bonds at the Si/SiO_2 interface. As the annealing temperature increases more oxygen atoms are introduced to Si nanocrystals, increasing the Si–O–Si bonds and number of the localized states. This explains the increase of the depth of the localized states E_0 after the thermal annealing in CO_2, as displayed in Fig. 6.

4. Conclusions

In summary, the PL properties of the silicon nanocrystals with thermal annealing in CO_2 were studied by the continuous and time-resolved PL. The PL intensity and decay time increase with increasing the annealing temperature. As the annealing temperature is up to 950 °C the PL intensity has a maximum value, which increases about a factor of 3 than that of the un-annealed sample. These observations are attributed to passivation of the nonradiative recombination centers by oxygen. Based on the emission energy dependence of the PL decay time, we suggest that PL decay in silicon nanocrystals involves recombination of the localized states at the Si/SiO_2 interface. The depth of the localized states increases as the annealing temperature increases. This increase is explained by the increase of the Si–O–Si bonds during the annealing process.

Acknowledgment

This project was supported in part by the National Science Council under the Grant nos. 93-2112-M-033-010 and NSC 93-2120-M-033-001.

Reference

[1] A.G. Cullis, L.T. Canham, P.D.J. Calcott, J. Appl. Phys. 82 (1997) 909.
[2] B. Gelloz, N. Koshida, J. Appl. Phys. 98 (2005) 123509.
[3] P.M. Fauchet, Mater. Today 8 (2005) 26.
[4] M. Sopinskyy, V. Khomchenko, Curr. Opin. Solid State Mater. Sci. 7 (2003) 97.
[5] S. Cheylan, R.G. Elliman, Appl. Phys. Lett. 78 (2001) 1912.
[6] K.S. Zhuravlev, A.M. Gilinsky, A.Yu. Kobitsky, Appl. Phys. Lett. 73 (1998) 2962.
[7] K. Sata, K. Hirakuri, J. Appl. Phys. 97 (2005) 104326.
[8] L.Y. Chen, W.H. Chen, F.C.N. Hong, Appl. Phys. Lett. 86 (2005) 193506.
[9] S. Cheylan, R.G. Elliman, Nucl. Instrum. Methods B 175 (2001) 422.
[10] M.L. Brongersma, A. Polman, K.S. Min, E. Boer, T. Tambo, H.A. Atwater, Appl. Phys. Lett. 72 (1998) 2577.
[11] T. Shimizu-Iwayama, T. Hama, D.E. Hole, I.W. Boyd, Nucl. Instrum. Methods B 230 (2005) 203.
[12] B.G. Fernandez, M. López, C. Garcia, A. Pérez-Rodríguez, J.R. Morante, C. Bonafos, M. Carrada, A. Claverie, J. Appl. Phys. 91 (2002) 798.
[13] M. López, B. Garrido, C. García, P. Pellegrino, A. Pérez-Rodríguez, J.R. Morante, C. Bonafos, M. Carrada, A. Claverie, Appl. Phys. Lett. 80 (2002) 1637.
[14] K.A. Brown, D.Q. Hu, W. Ho, J. Chem. Phys. 104 (1996) 2358.
[15] B. Deal, J. Electrochem. Soc. 110 (1963) 527.
[16] E. Cohn, M.D. Sturge, Phys. Rev. B 25 (1982) 3828.
[17] M.V. Wolkin, J. Jorne, P.M. Fauchet, G. Allan, C. Delerue, Phys. Rev. Lett. 82 (1999) 197.
[18] I. Vasiliev, J.R. Chelikowsky, R.M. Martin, Phys. Rev. B 65 (2002) 121302.
[19] M. Strassburg, M. Dworzak, H. Born, R. Heitz, A. Hoffmann, M. Barteis, K. Lischka, D. Schikora, J. Christen, Appl. Phys. Lett. 80 (2002) 473.